

GA-A26110

MEASUREMENTS OF THE INTERNAL MAGNETIC FIELD ON DIII-D USING INTENSITY AND SPACING OF THE MOTIONAL STARK MULTIPLY

by
N.A. PABLANT, K.H. BURRELL, C.T. HOLCOMB,
R.J. GROEBNER, and D.H. KAPLAN

MAY 2008



DISCLAIMER

This report was prepared as an account of work sponsored by an agency of the United States Government. Neither the United States Government nor any agency thereof, nor any of their employees, makes any warranty, express or implied, or assumes any legal liability or responsibility for the accuracy, completeness, or usefulness of any information, apparatus, product, or process disclosed, or represents that its use would not infringe privately owned rights. Reference herein to any specific commercial product, process, or service by trade name, trademark, manufacturer, or otherwise, does not necessarily constitute or imply its endorsement, recommendation, or favoring by the United States Government or any agency thereof. The views and opinions of authors expressed herein do not necessarily state or reflect those of the United States Government or any agency thereof.

MEASUREMENTS OF THE INTERNAL MAGNETIC FIELD ON DIII-D USING INTENSITY AND SPACING OF THE MOTIONAL STARK MULTIPLET

by
N.A. PABLANT,* K.H. BURRELL, C.T. HOLCOMB,[†]
R.J. GROEBNER, and D.H. KAPLAN

This is a preprint of a paper to be presented at the 17th
Topical Conference on High Temperature Plasma
Diagnostics, May 11-15, 2008, in Albuquerque, New
Mexico, and to be published in the *Proceedings*.

*University of California-San Diego, California

[†]Lawrence Livermore National Laboratory, Livermore, California

Work supported by
the U.S. Department of Energy
under DE-FC02-04ER54698, DE-FG02-07ER54917
and DE-AC52-07ER27344

GENERAL ATOMICS PROJECT 30200
MAY 2008



ABSTRACT

We describe a version of a motional Stark effect diagnostic based on the relative line intensities and spacing of Stark split D_α emission from the neutral beams. This system, named B-Stark, has been recently installed on the DIII-D tokamak. To find the magnetic pitch angle, we use the ratio of the intensities of the π_3 and σ_1 lines. These lines originate from the same upper level and so are not dependent on the population levels. In future devices, such as ITER, this technique may have advantages over diagnostics based on motional Stark effect polarimetry (MSE). We have done an optimization of the viewing direction for the available ports on DIII-D to choose the installation location. With this placement, we have a near optimal viewing angle of 59.6 deg from vertical. All hardware has been installed for one chord, and we have been routinely taking data since January 2007. We fit the spectra using a simple Stark model in which the upper level populations of the D_α transition are treated as free variables. The magnitude and direction of the magnetic field obtained using this diagnostic technique compare well with measurements from MSE polarimetry and EFIT.

I. INTRODUCTION

This paper describes a diagnostic, B-Stark, recently installed on the DIII-D tokamak at General Atomics. This system is a version of a motional Stark effect diagnostic and measures both the magnitude and direction of the internal magnetic field. These measurements are made using the relative line intensities and spacing of Stark split D_α emission from the neutral beams. This differs from motional Stark effect polarimetry (MSE) which only measures the direction of the field and relies on the polarization properties of the D_α light.

The ability to measure the direction of the internal magnetic field has led to important advances in tokamak research. In particular, these measurements have allowed a better understanding of magnetic shear and the mechanisms behind improved confinement modes, such as H-Mode [1]. MSE polarimetry is now considered to be an essential diagnostic in tokamak and stellarator systems.

Measurements of the magnitude from the magnetic field can provide additional information for magnetic equilibrium reconstruction codes such as EFIT [2]. These codes solve the Grad-Shafranov equation, and with several chords the ff' term can be measured locally. This, in turn, can lead to better understanding of poloidal currents.

The B-Stark diagnostic may have additional advantages over MSE polarimetry in devices with high densities and temperatures, such as ITER. Under these conditions coatings on plasma facing mirrors are expected. These coatings may interfere with MSE polarimetry by causing changes in the polarization direction of light incident on the mirror [3]. The B-Stark diagnostic is not sensitive to the polarization direction. It is, however, sensitive to polarization dependent transmission. There is a simple calibration procedure using a beam into gas shot that can be used to correct for this effect.

Diagnostics to measure the direction of the magnetic field based on the Stark intensities have been developed and used on TEXTOR [4] and JET [5]. Both of these systems had non-optimal viewing locations on the midplane, which required them to use additional information to make the measurement. In addition, both of these experiments measured the total π and σ intensities, requiring the assumption of statistical upper level populations.

Measurements of $|B|$ based on the Stark spacing have been made in JET [5][6] and in the MST reversed field pinch [7].

This new system installed at DIII-D has two main advantages over the previous diagnostics; it has a near optimal viewing direction, and DIII-D has an excellent MSE polarimetry system [8] with which the B-Stark measurements can be compared.

A similar diagnostic system has been proposed for ITER [9].

II. THEORY

This diagnostic relies on the emission spectrum from the neutral heating beams on DIII-D. We are interested in the light from the D_{α} ($n=3$ to $n=2$) transition, around $\lambda_0 = 6561.0 \text{ \AA}$. Stark splitting of the energy levels occurs when the atom is exposed to an electric field.

For the deuterium atoms injected into the plasma by the neutral beams, there are two sources of electric fields. There is a Lorentz electric field produced by the particle's motion across the magnetic field, and a radial electric field from the plasma. This electric field can be written as $\mathbf{E} = \mathbf{v}_b \times \mathbf{B} + \mathbf{E}_r$.

For our diagnostic, typical $\mathbf{v}_b \times \mathbf{B}$ fields will have a magnitude of $\sim 4 \times 10^6 \text{ V/m}$, while typical \mathbf{E}_r fields are around $5 \times 10^4 \text{ V/m}$. We therefore ignore the \mathbf{E}_r field in our calculations. In certain high performance plasmas the \mathbf{E}_r field can be as large as $2 \times 10^5 \text{ V/m}$ [8], and a calculation including \mathbf{E}_r is needed.

The effect of Zeeman splitting in calculating the spacing between the lines can be ignored, and a linear Stark effect is assumed [5]. For the linear Stark effect the spacing between the lines can be written as $\Delta\lambda = \lambda_0^2 (3/2)(ea_0/hc) |\mathbf{E}|$ [9].

The lines are polarized parallel to the electric field for $\Delta m = 0$ (π transitions), and polarized perpendicular to the field for $\Delta m = \pm 1$ (σ transitions). The intensity of the emission is spatially anisotropic, and the ratio of π to σ light can be used to find the direction of the electric field. In general this requires the level populations of the $n = 3$ states to be known. Two sets of lines, $\pi \pm 3/\sigma \pm 1$, originate from the same upper level removing the dependence on the level populations [9]. The intensity ratio of these lines is

$$\frac{I_{\pi}}{I_{\sigma}} = \frac{2 \sin^2 \Theta}{1 + \cos^2 \Theta} A T_f, \quad (1)$$

where Θ is the angle between the viewing direction and the electric field, A is the constant ratio of the transition probabilities, and T_f the the π to σ transmission ratio for the optical system.

The angle Θ can be related to the magnetic field through the Lorentz field vector and the viewing direction. The line intensity ratio in Eq. (1) can then be related to the magnetic field ratio B_{θ}/B_y .

$$\frac{2AT_f - \frac{I\pi}{I_\sigma}}{2AT_f + \frac{I\pi}{I_\sigma}} = \frac{\left(\ell_z + \ell_y \frac{B_\theta}{B_y}\right)^2}{1 + \left(\frac{B_\theta}{B_y}\right)^2} . \quad (2)$$

Here the \hat{x} direction is taken to be along the beam and the \hat{z} direction is taken to be vertical. ℓ_y and ℓ_z are the y and z components of the unit viewing vector. B_θ/B_T can be related to B_θ/B_y though the known angle between the beam and the toroidal direction at the viewing location. B_θ and B_T are the poloidal and toroidal components of the magnetic field.

III. EXPERIMENTAL SETUP

For the B-Stark diagnostic, the viewing direction with respect to the neutral beam is important for several reasons.

From Eq. (1) it can be seen that the sensitivity of the ratio to changes in Θ is maximized at 62.1 deg. This is the optimal viewing angle from the electric field, which in DIII-D is nearly vertical.

For Doppler separation of the beam emission from the background D_α emission, the viewing direction must be away from beam perpendicular. In order to achieve good radial resolution, the view must be tangent to the toroidal direction at the viewing location. To maximize signal levels, the viewing location must be outside of the magnetic axis where the neutral beam intensity is greatest. Lastly, a view crossing more than one beam allows better calibration and consistency testing.

The final port chosen for the B-Stark installation allows views that cross two of the neutral beams, with angles of 57.8 deg and 64.9 deg, and have an angle of 59.9 deg from the vertical (Fig. 1). The radial resolution, calculated from the change in major radius over the neutral beam viewing volume, is 1–3 cm.

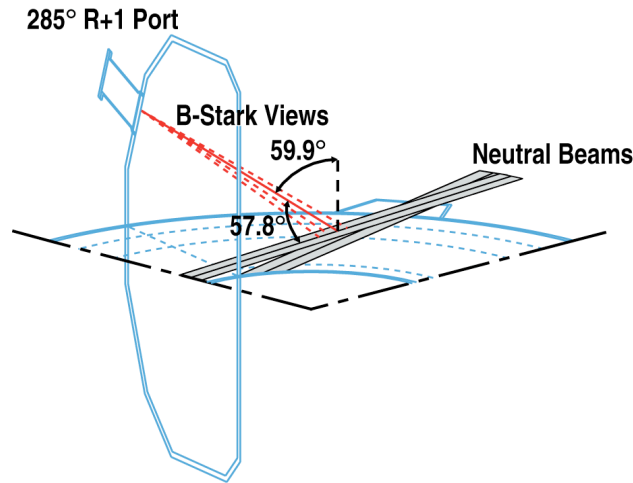


Fig. 1. (Color On-line ONLY) B-Stark diagnostic geometry. Cross sections of the DIII-D vessel at the midplane and at a toroidal angle of 285 deg are shown. The B-Stark chords cross the 330 deg left and 330 deg right neutral beams. The angle between the 330 deg left neutral beam and the B-Stark chord is 57.8 deg. The angle between the vertical direction and the B-Stark chord is 59.9 deg. The neutral beams have a width of ~20 cm and a height of ~40 cm.

In order to maximize light throughput while maintaining narrow slit widths, custom fiber bundles were designed that are packed into two square ferrules at the plasma viewing end and packed into a line on the spectrometer end. The bundles each have 38 fibers with $200\text{ }\mu\text{m}$ core diameter. The two ends of the fiber bundle can be arranged to act as a single chord, to maximize light gathering, or as separate chords.

The installed viewing optics are $f/2.3$ to allow for future upgrades to a faster spectrometer. A lens mask was installed to reduce geometrical Doppler broadening due to the change in viewing angle across the lens. We are using an available SPEX 3/4 – m Czerny-Turner spectrometer ($f/6.8$) coupled to a PixelVision CCD camera with $12\text{ }\mu\text{m}$ pixel pitch. The top and bottom halves of the chip are summed vertically, and pixels binned by two, resulting in 326 channels. This system has a dispersion of $\sim 0.14\text{ }\text{\AA}/\text{channel}$, and an instrumental response with a FWHM of $\sim 0.4\text{ }\text{\AA}$.

An in-vessel calibration is performed to find the viewing and effective lens locations, and to characterize the intensity response.

IV. SPECTRUM

The D_α spectrum is made up of emission from several sources. The B-Stark diagnostic relies on emission from the neutral beams; however background emission must also be taken into account in order to properly fit the spectrum.

The neutral beams on DIII-D inject deuterium atoms at three energies due to molecular deuterium in the ion source [10]. In addition there is a continuum of energies between the third and half components due to molecular D_3^+ breaking into $D_2^+ + D$ partway through acceleration in the ion source. The D_α emission from each of these components, as well as the continuum, is Stark split and Doppler shifted.

For typical values of the magnetic field and beam energy, emission from the full component is spectrally separated while the half and third components overlap. The separation between the Stark lines for the full component is $\sim 1.0 \text{ \AA}$.

The width of the beam emission lines is dominated by geometrical Doppler broadening due to the divergence of the neutral beam [11]. This causes a Doppler broadening of the beam emission with a FWHM of $\sim 1.6 \text{ \AA}$. This line width is greater than the Stark spacing, and makes the individual lines difficult to distinguish.

There are a number of other sources that contribute to the D_α spectrum. There is D_α and H_α emission from neutral deuterium and hydrogen in the edge, both of which are Zeeman split. There is emission from re-neutralized deuterium around the neutral beam, which is Doppler shifted due to the plasma rotation and thermally broadened. Lastly, there are impurity lines from the beams and the plasma.

Most of the components in the spectra are beam dependent, reducing the effectiveness of time slice subtraction in removing the background emission.

V. RESULTS

A spectral fit is performed to extract the intensity ratio and line spacing (Fig. 2). The fitting is done using a modified version of the non-linear least squares fitting package, CERFIT [12,13].

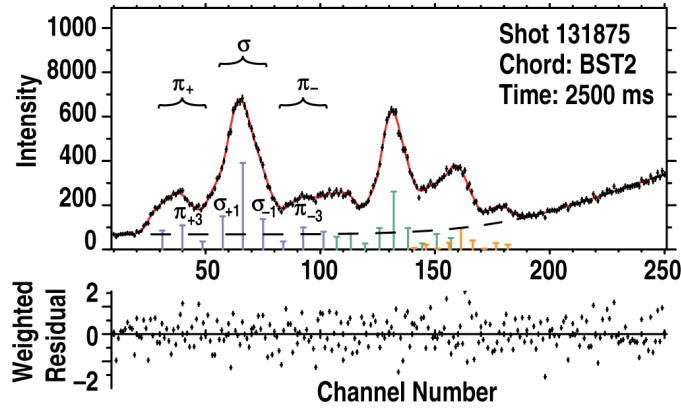


Fig. 2. (Color On-line ONLY) Fit of a B-Stark spectra for shot 131875 at 2500 ms. Data is shown as crosses, the fit is shown as a solid line. Here the background is made up of one Gaussian and a constant term. The weighed residual is found from the difference between the data and the fit, divided by the standard deviation of the data. The reduced chi-squared is 1.1.

The line spacing is assumed to be described by a linear Stark model. The fit variables in this model are the upper state level populations, beam velocity, effective electric field, and the intensity ratio of the π to σ components. We allow each of the beam components to have unique upper state populations. The background is described using Gaussians and up to a quadratic polynomial. In addition the spectrometer fiducial (central wavelength) is given as a fit variable.

Shots where the neutral beams are injected into a low density gas (beam into gas) are used to find the line profiles and to calibrate the B-Stark system.

A spectrum produced by firing a beam into gas shot without magnetic field is used to find the spectral profile for the lines from each beam energy component and to find an instrumental profile to use for the background lines.

In addition to the in-vessel spatial calibration, a beam into gas with toroidal field shot is used to determine in-situ the viewing direction and the ratio of transmission of π to σ light. The magnetic field in these shots is purely toroidal and is assumed to have a $1/R$ dependence. To obtain both the direction and transmission factor, measurements from two beams at different angles are necessary.

The B-Stark measurements compare well with values taken from EFIT using MSE polarimetry data, for both $|B|$ and B_θ/B_T . In Fig. 3 we show B-Stark measurements from shot 131875. Measurements were taken with a time resolution of 10 ms. The major radius of the viewing location was found using the in-vessel calibration, while the viewing direction and transmission factor were found using a beam into gas calibration. The error in the measurement of $|B|$ is 0.015 T or 1% and for the measurement of B_θ/B_T the error is 0.12 or 10%. These errors are found from the standard deviation of the final measurements over a period where the parameters are expected to be constant (around 2500 ms). The discrepancy in $|B|$ changes from ~ 0.08 T to ~ 0.05 T over the time range analyzed. A number of shots have been analyzed and the discrepancy in $|B|$ is not always seen.

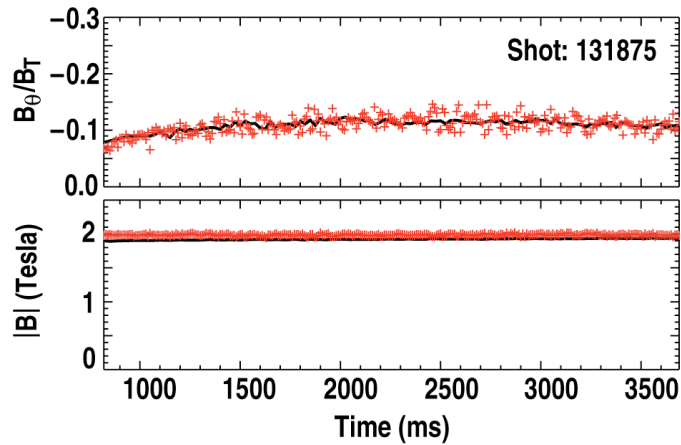


Fig. 3. (Color On-line ONLY) B_θ/B_T and $|B|$ versus time for shot 131875. B-Stark measurements (crosses) are taken every 10 ms. EFIT with MSE polarimetry results (solid line) are calculated every 25 ms.

The accuracy of these measurements are dependent on the quality of the spectral fits. The main difficulties in getting good fits are the wide line profiles due to the beam divergence, poor signal due to the need for high spectral resolution, and a complicated background.

VI. FUTURE PLANS

Work is continuing to improve the fitting model. In addition we plan to evaluate the use of an atomic code [14] to calculate the expected level populations. This will reduce the number of fit parameters, resulting in better accuracy in determining the π to σ ratio.

There are several planned hardware upgrades including a new camera that will allow an expansion to multiple chords and a faster spectrometer in order to get better signal levels.

REFERENCES

- [1] K. H. Burrell, *Phys. Plasmas* **4**, 1499 (1997).
- [2] L. Lao, J. Ferron, R. Groebner, W. Howl, H. John, E. Strait, and T. Taylor, *Nucl. Fusion* **30**, 1035 (1990).
- [3] A. Malaquias, M. von Hellermann, S. Tugarinov, P. Lotte, N. Hawkes, M. Kuldkepp, E. Rachlew, A. Gorshkov, C. Walker, A. Costley, et al., *Rev. Sci. Inst.* **75**, 3393 (2004).
- [4] K. Jakubowska, M. De Bock, R. Jaspers, M. G. von Hellermann, and L. Shmaenok, *Rev. Sci. Inst.* **75**, 3475 (2004).
- [5] W. Mandl, R. C. Wolf, M. G. von Hellermann, and H. P. Summers, *Plasma Phys. & Controlled Fusion* **35**, 1373 (1993).
- [6] R. Wolf, L. Eriksson, M. Hellermann, R. Koenig, W. Mandl, and F. Porcelli, *Nucl. Fusion* **33**, 1835 (1993).
- [7] D. J. D. Hartog, D. Craig, D. A. Ennis, G. Fiksel, S. Gangadhara, D. J. Holly, J. C. Reardon, V. I. Davydenko, A. A. Ivanov, A. A. Lizunov, et al., *Rev. Sci. Inst.* **77**, 10F122 (pages 8) (2006), URL <http://link.aip.org/link/?RSI/77/10F122/1>.
- [8] C. T. Holcomb, M. A. Makowski, R. J. Jayakumar, S. A. Allen, R. M. Ellis, R. Geer, D. Behne, K. L. Morris, L. G. Seppala, and J. M. Moller, *Rev. Sci. Inst.* **77**, 10E506 (pages 3) (2006), URL <http://link.aip.org/link/?RSI/77/10E506/1>.
- [9] M. von Hellermann, M. de Bock, R. Jaspers, K. Jakubowska, R. Barnsley, C. Giroud, N. Hawkes, K. Zastrow, P. Lotte, R. Giannella, et al., *Rev. Sci. Inst.* **75**, 3458 (2004).
- [10] B. W. Rice, K. H. Burrell, L. L. Lao, and Y. R. Lin-Liu, *Phys. Rev. Lett.* **79**, 2694 (1997).
- [11] B. H. Bransden and C. Joachain, *Physics of Atoms and Molecules* (Pearson Education Limited, 2003), 2nd ed.
- [12] R. Hong and H. K. Chiu, *Fusion Engineering*, 2002. 19th Symposium on pp. 40–43 (2002).
- [13] H. Chiu, *Fusion Tech.* **34**, 564 (1998).
- [14] R. P. Seraydarian, K. H. Burrell, N. H. Brooks, R. J. Groebner, and C. Kahn, *Rev. Sci. Inst.* **57**, 155 (1986).
- [15] D. S. Bunch, D. M. Gay, and R. E. Welsch, *ACM Trans. Math. Software* **19**, 109 (1993).
- [16] M. Gu, *AIP Conference Proceedings* **730**, 127 (2004).

ACKNOWLEDGMENT

Work supported by the U.S. Department of Energy under DE-FC02-04ER54698, DE-FG02-07ER54917 and DE-AC52-07NA27344.